



Influence of electrode configuration on electrokinetic-enhanced persulfate oxidation remediation of PAH-contaminated soil

Hongting Xu^{1,2} · Long Cang^{1,3} · Yue Song¹ · Jiangli Yang^{1,3}

Received: 28 February 2020 / Accepted: 30 July 2020 / Published online: 7 August 2020
© Springer-Verlag GmbH Germany, part of Springer Nature 2020

Abstract

Electrokinetic (EK) remediation combined with in situ chemical oxidation (ISCO) can be applied to low permeability organic contaminated soil. However, the effects of electrode configuration on EK-oxidation remediation remain unclear. In this study, EK-ISCO remediation of real polycyclic aromatic hydrocarbon (PAH)-contaminated soil under different electrode configurations was conducted. The results showed that increasing the number of anodes and electrode pairs in one-dimensional (1D) and two-dimensional (2D) electrode configuration was conducive to migration of oxidants into the system. The change in soil pH after remediation in 2D electrode configuration was not obvious, but the increase of soil electrical conductivity (EC) was higher than that of the 1D electrode configuration. The removal rates of PAHs in 2D electrode configurations (35.9–40.9%) were relatively higher than those of the 1D electrode configurations (0.54–31.6%), and the hexagonal electrode configuration yielded the highest pollutant removal efficiency, reaching 40.9%. The energy consumption under 2D electrode configuration was smaller than that under 1D electrode configuration, and the energy consumption of per gram removed PAHs in the hexagon configuration ($66.74 \text{ kWh (g PAHs)}^{-1}$) was lowest in all electrode configurations. Overall, the results of this study suggest that 2D electrode configuration is better than 1D and hexagonal electrode configuration is an optimal electrode configuration.

Keywords Electrokinetic · Chemical oxidation · Electrode configuration · Persulfate · PAHs · Soil

Introduction

With the rapid development of industry, soil contamination by organic pollutants has become a serious environmental problem. A great variety of technologies have been developed for the remediation of the contaminated soils, including physical (e.g., thermal desorption (Zhao et al. 2019) and soil washing (Yang et al. 2006; Dermont et al. 2008)), chemical (e.g., chemical oxidation (Ferrarese et al. 2008; Gryzenia et al. 2009; Rastogi et al. 2009a; Liang et al. 2008a)), and biological processes (e.g., microbial remediation (Juhasz and Naidu

2000; Bento et al. 2005)). Among these technologies, in situ chemical oxidation (ISCO) is a widely used technology for soil and groundwater remediation because of its wide applicability, relatively fast treatment, simplicity of operation, and cost-effectiveness (Wang and Wang 2018; Rastogi et al. 2009b; Tsitonaki et al. 2010). The main principle of ISCO involves the introduction of a chemical oxidant into the subsurface to transform organic contaminants into less harmful chemical species. Many oxidants, such as persulfate, permanganate, and hydrogen peroxide, have been widely used in ISCO for remediation of organic contaminated soil and groundwater. However, the application of ISCO in low permeability soils is limited because of the difficult delivery of oxidants in such soils (Yukselen-Aksoy and Reddy 2012; Fan et al. 2014a).

In recent years, researchers have combined electrokinetic (EK) remediation with ISCO to remediate organic contaminated soil. In this method, the oxidant can be transported into soil by electromigration and electroosmotic flow. Yang and Yeh (2011) found that the EK process greatly enhanced the transport of injected persulfate from the anode reservoir to the cathode reservoir by means of electroosmotic flow, aiding in

Responsible Editor: Vitor Pais Vilar

✉ Long Cang
canglong@issas.ac.cn

¹ Key Laboratory of Soil Environment and Pollution Remediation, Institute of Soil Science, Chinese Academy of Sciences, Nanjing 210008, China

² Geological Survey of Jiangsu Province, Nanjing 210018, China

³ University of Chinese Academy of Sciences, Beijing 100049, China

situ chemical oxidation of trichloroethylene (TCE). Yukselen-Aksoy and Reddy (2012) investigated electrokinetically enhanced persulfate delivery and oxidation of tetrachlorobiphenyl (PCB 44) in two diverse low permeability soils: artificially contaminated kaolin and glacial till soil. They found that the activation of persulfate improved the oxidation of PCB in kaolin, but the effects in glacial till were insignificant. Fan et al. (2014b) selected persulfate as an oxidant for enhanced EK to remediate PCBs polluted soil and found that persulfate was successfully delivered from the cathode toward the anode by EK and that the highest degradation rate of PCBs was 38.0%. These studies confirmed the feasibility of treating soil using EK combined with ISCO. However, most EK-enhanced ISCO remediation experiments have been conducted using a one-dimensional (1D) electrode setting (equal number of anodes and cathodes), while few studies have focused on the influence of different electrode configurations on the transport of oxidation and removal of organic pollutants. In fact, the electrode configuration is very important to the application of EK-ISCO remediation because it affects the electrode installation cost, remediation efficiency, and operation time (Alshawabkeh et al. 1999; Kim et al. 2014).

The electric field could be 1D or two-dimensional (2D) (unequal number of anodes and cathodes) depending on the electrode array. Generally, electrode pairs are adopted to generate a 1D electrical field, while configurations of regular polygons (e.g., triangular, square, hexagonal) are used to produce 2D electric fields (Alshawabkeh et al. 1999). There have been few studies of 2D electrokinetic remediation, especially in field applications. Maini et al. (2000) first studied the EK remediation of a historically contaminated soil under a hexagonal 2D electrode configuration. Turer and Genc (2005) then studied the effects of electrode geometry on the removal efficiency by constructing an octagonal electrode configuration for use in EK remediation experiments and found corresponding overall efficiencies of lead, zinc, and copper removal from soil of 29%, 18%, and 18%, respectively. These values were lower than those obtained when a plate electrodes arrangement was used (32%, 37%, and 31%, respectively). Kim et al. (2012b) studied the effects of 1D electrode configurations on the in situ electrokinetic remediation of As, Cu, and Pb contaminated soils in pilot sites. The heavy metals removal effect was not ideal, which may have been because of the soil heterogeneity and groundwater level. At present, most of the studies focused on the effects of electrode configurations on the removal of heavy metals and base cation (Kim et al. 2012a; Krcmar et al. 2018), but the effects of electrode configurations on the migration and removal of organic pollutants were not yet clear.

Recently, the group of Rodrigo MA have done a lot of research about the effect of electrode configuration on EK remediation of organic contaminated soil. These studies

mainly focused on the polarity reversal of the anodes and cathodes (Lopez-Vizcaino et al. 2017; Barba et al. 2017; Mena et al. 2016), linear rows of electrodes (Risco et al. 2016a, 2016b), and surrounding electrode arrangements (Risco et al. 2016c, 2016d). These results indicated that the above electrode configurations improved the removal efficiency of organic pollutants during electrokinetic soil flushing (EKSF) remediation. However, the comparison of different electrode configurations on the removal efficiency of organic pollutants by EK-oxidation remediation was not studied in these papers and the impact mechanism of different electrode configurations was not clear. Therefore, further study is needed to determine how to further improve EK efficiency under different electrode configurations, especially during EK-oxidation remediation for treatment of organic polluted soil.

In this study, PAH-contaminated soil was used as the research object, persulfate was used as an oxidant, and different electrode configurations were set up in the EK-oxidation remediation. Oxidant transport, PAH removal rates, and changes in soil pH and EC after restoration, as well as energy consumption, were then compared to determine the impact of electrode configuration.

Materials and methods

Tested soil

The tested soil (*Alfisol*) was collected from a gas plant polluted with PAHs in Nanjing, China, air-dried, mixed, and sieved through a 20-mesh sieve. The soil pH (soil to water ratio = 1:5) was 8.42 and the electrical conductivity (EC) was 299 $\mu\text{S cm}^{-1}$. The contents of clay, silt, and sand in the soil were 30.9%, 34.1%, and 35.0%, respectively. The mineralogy of the soil was 28% quartz, 27% feldspar, 22% water mica, 6% kaolinite, 6% roseite, 5% gibbsite, 4% chlorite, and 2% calcite. The soil organic matter (OM) and cation exchange capacity (CEC) was 9.35 g kg^{-1} and 18.97 cmol kg^{-1} , respectively. The total PAH concentration in contaminated soil was 6.69 mg kg^{-1} , and the initial concentrations of the 16 PAHs are shown in Table 1. The analysis methods of soil properties were showed in the “Analytical methods” section.

EK experiments

The schematic diagram of electrode configurations is shown in Fig. 1. The electrical treatment tank was a PVC cylinder ($R = 25$ cm, $H = 10$ cm) containing about 4 kg of dry soil. Different electrode configurations could be arranged within the treatment tank according to experimental requirements. The electrolytic cell was a hollow PVC cylinder ($\varnothing = 2$ cm, $h = 11.5$ cm) with water-permeable holes on the surface, and the outer layer was covered with a nylon net of 200 mesh to

Table 1 Initial PAH concentration and removal rates of PAHs after different treatments

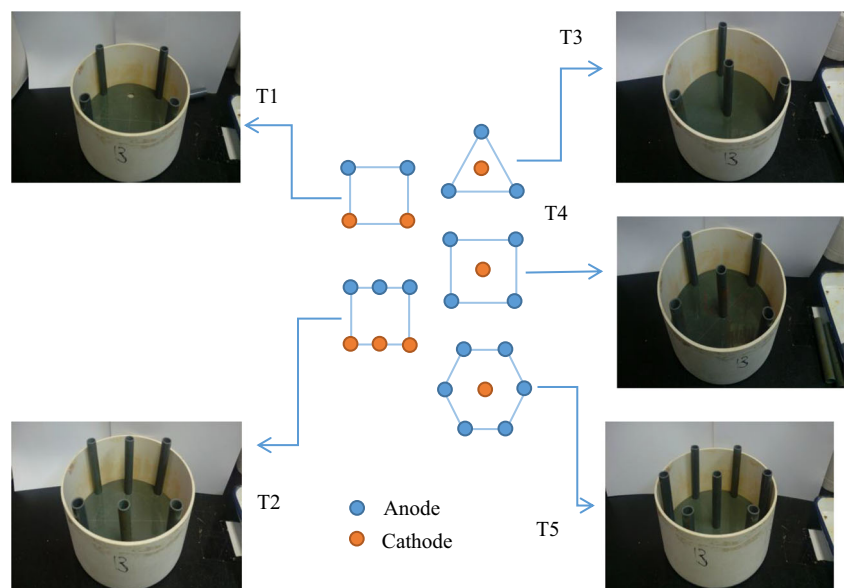
PAHs	Initial concentration (µg/kg)	Removal rates				
		T1 (%)	T2 (%)	T3 (%)	T4 (%)	T5 (%)
Naphthalene	183	-23.6	40.3	66.7	45.7	34.3
Acenaphthylene	167	-5.11	39.5	43.0	47.1	43.3
Acenaphthene	27	-2.09	42.3	51.5	43.5	43.6
Fluorene	62	-35.5	-7.4	-7.1	-3.4	-6.0
Phenanthrene	709	12.6	37.2	40.9	47.0	44.4
Anthracene	122	-9.22	15.2	23.9	36.6	40.3
Fluoranthene	1150	13.4	30.9	35.7	42.2	40.7
Pyrene	882	11.7	39.8	41.1	47.6	48.6
Benz[a]anthracene	445	4.34	38.2	34.5	40.5	46.0
Chrysene	512	1.84	31.0	40.6	40.9	41.8
Benzo[b]fluoranthene	559	-7.01	23.7	32.4	27.6	40.6
Benzo[k]fluoranthene	460	-14.8	31.2	27.9	31.3	36.3
Benzo[a]pyrene	426	-3.21	33.8	34.5	39.8	43.6
Indeno(1,2,3-c,d)pyrene	444	-12.6	26.9	33.6	31.4	38.1
Dibenz(a,h)anthracene	107	-59.2	-37.1	-29.8	-25.7	-21.3
Benzo[g,h,i]perylene	440	-2.97	33.9	39.0	37.8	42.6
Total	6694	0.54	31.6	35.9	38.7	40.9

prevent soil from entering the electrolyte. Ruthenium oxide coated titanium (Ti/RuO₂) alloy sheets (1 cm × 15 cm) connected to the DC power source were used as electrodes and were placed in the electrolytic cells. The voltage gradient was set to 1 V cm⁻¹. Deionized water was used to saturate the soil matrix before the experiment. The total porosity, hydraulic conductivity, and density of the soil column were 55.4%, 4.6 × 10⁻⁵ cm s⁻¹, and 2.61 g cm⁻³, respectively.

Five experiments (T1–T5) were conducted. T1 and T2 were 1D electrode configurations and the anode and the

cathode had one-to-one correspondence. T3, T4, and T5 were 2D electrode configurations, with the cathode located at the center and the anodes arranged around the cathode in triangle (T3), square (T4), and hexagon (T5) configurations. According to the previous study (Fan et al. 2014a, 2014b), persulfate solution can migrate to cathode by electroosmotic flow and reducibility in the cathode would cause loss of the persulfate, so the 20 ml 20% Na₂S₂O₈ solution (Fan et al. 2014b; Xu et al. 2020) was added in the anode cells by gravity per treatment group on days 1, 4, 6, and 8. Due to the different

Fig. 1 Schematic diagram of electrode configurations (T1, two pairs of electrodes; T2, three pairs of electrodes; T3, triangle electrode configuration; T4, square electrode configuration; T5, hexagon electrode configuration)



number of anodes in T1~T5, the amount of $\text{Na}_2\text{S}_2\text{O}_8$ solution added in every anode cells of different treatments was different.

The sampling plot is shown in Fig. 2. The sampling areas set in T1 and T2 were divided into 12 equal parts according to the distance from the electrodes and the strength of the electric field and denoted A1, A2, A3, B1, B2, B3, A1', A2', A3', B1', B2', and B3', respectively. Soil solution samplers were buried in each sampling area before the trials (Zhou et al. 2007) and were in soil all the time of experiments. The sampling areas set in T3, T4, and T5 were divided into concentric circles outward from the cathode with soil solution samplers isometrically buried on each concentric circle. The EK treatment lasted for 10 days and the electrical currents were recorded during the test. Soil solutions were collected on days 1, 3, 5, 8, and 10, and the pH and $\text{S}_2\text{O}_8^{2-}$ concentrations were measured accordingly.

After the EK experiment, the soil was cut into 12 equal sections in T1 and T2, and the symmetric soils were prepared as a mixture. In T3, T4, and T5, the soil on the same concentric

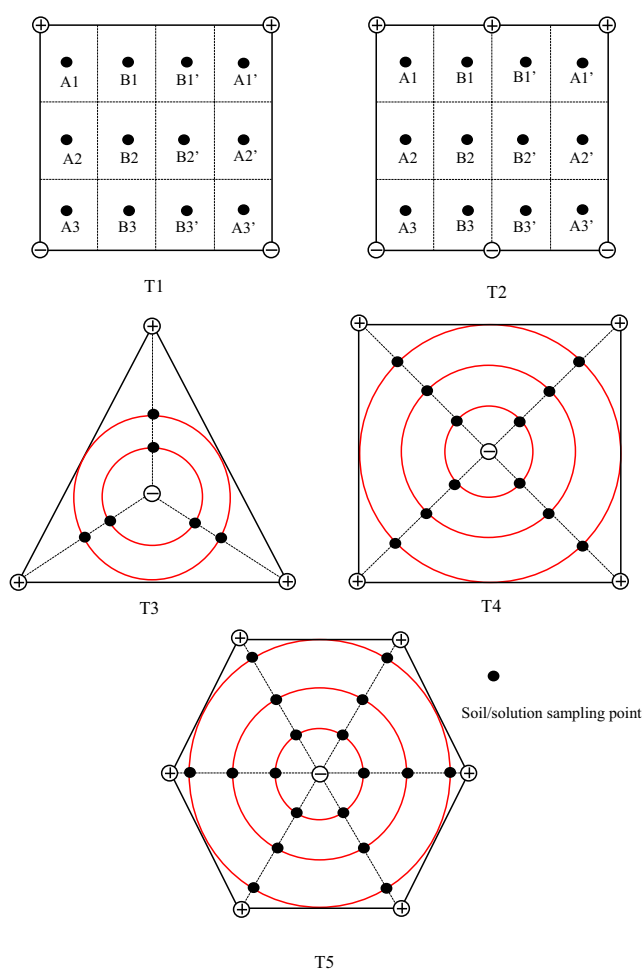


Fig. 2 Soil/solution sampling plot

circle was prepared as a mixed sample. The pH, EC, and PAH concentrations of each part were then determined.

Analytical methods

Electrical current was directly recorded using an automatic acquisition system (ITECH Electronic Co., Ltd., IT6322A, Beijing, China). Soil pH, EC, OM, and CEC were analyzed using usual analytical methods (Lu 2000). The pH and EC of soil and soil solutions were measured using a pH meter (Shanghai REX Instrument Factory, pHS-3B, China) and an EC meter (Shanghai REX Instrument Factory, DDS-11A, China), respectively (soil to water ratio = 1:5). Soil CEC and OM were analyzed by NH_4AcO exchange method and dichromate oxidation method, respectively. For the determination of soil particle composition, 20 ml 15% H_2O_2 and 10 ml 0.2 mol L^{-1} HCl were successively added to 5.0-g soil to remove soil organic matter and carbonate. Then, deionized water (DIW) was used to rinse the suspension and to remove redundant Ca^{2+} and Cl^- . At last, the suspension was determined using a laser particle size analyzer (Beckman Coulter, Inc., LS13320, USA).

The concentrations of $\text{S}_2\text{O}_8^{2-}$ in solution were determined by UV spectrophotometry (Liang et al. 2008b). Briefly, 100-fold diluted soil solution (0.1 mL) was added to a colorimetric tube (25 mL), after which 166.7 g L^{-1} KI (15 mL) and 12.5 g L^{-1} NaHCO_3 (10 mL) were added. The contents were then mixed and allowed to react (15 min). Finally, the absorbance was measured with a spectrophotometer (Shimadzu, UV-2700, Japan) at a wavelength of 352 nm.

To analyze the PAHs in soil, 5.0 g of air-dried soil was extracted twice with *n*-hexane/acetone (1:1) by pressurized liquid extraction using an ASE (100 °C) (ThermoFisher Technology Corporation, ASE350, USA) (Pies et al. 2008). All extracts were concentrated to approximately 1 mL under a gentle stream of N_2 , after which the samples were analyzed for PAHs by gas chromatography-mass spectrometry (ThermoFisher Technology Corporation, Trace 1300&ISQ, USA) (Pies et al. 2008; Tang et al. 2005) coupled with a TG-5 MS $30 \text{ m} \times 0.25 \text{ mm} \times 0.25 \text{ }\mu\text{m}$ column (ThermoFisher Technology Corporation, USA). The temperature of the injector was set at 280 °C. The carrier gas was helium at a flow rate of 1.0 mL min^{-1} , while the oven was programmed to increase from 40 (held for 4 min) to 310 °C (held for 10 min) at a rate of $8 \text{ }^\circ\text{C min}^{-1}$. The mass spectrometer was operated under a selected ion scan mode. The rates of recovery were from 86.1–107%.

Data analysis and charting

The current was recorded directly by the power supply at a time interval of 1 h, and one data point was taken every 5 h

while drawing. The energy consumption was calculated according to the following formula (Sawada et al. 2004):

$$E = \int \frac{VIdt}{W}$$

where E is the power consumption (kWh t^{-1}); W is the soil weight (t); V is the voltage between electrodes (V); I is the current (A) and t is the time (h). Data analysis was conducted using Microsoft Excel 2010. The charts involved in this article were made using Origin 8.6.

Results and discussion

Change of electrical current

The current change in each treatment is shown in Fig. 3. The electrical current across the soil matrix was highly relative to the concentration of mobile ions in the system (Acar and Alshawabkeh 1993; Yu and Neretnieks 1997; Fu et al. 2017). When no external ions were added into the electrolyte, the electrical current was expected to be at a low level (Saichek and Reddy 2003; Zhou et al. 2005). As shown in Fig. 3, the initial currents of the five treatments were at the same level, after which the current increased continuously with the experiment until reaching a maximum of 1.00 A (T4). The increase in current was due to the continuous accumulation of total ions in the system caused by the regular addition of persulfate. Higher ion concentrations corresponded to higher electrical conductivity, so that the current increased (Zhang et al. 2018). At the same time, the experimental currents of the five treatments exhibited periodic fluctuations because of the regular supplementation of the persulfate. The electrical current in T5 increased rapidly from

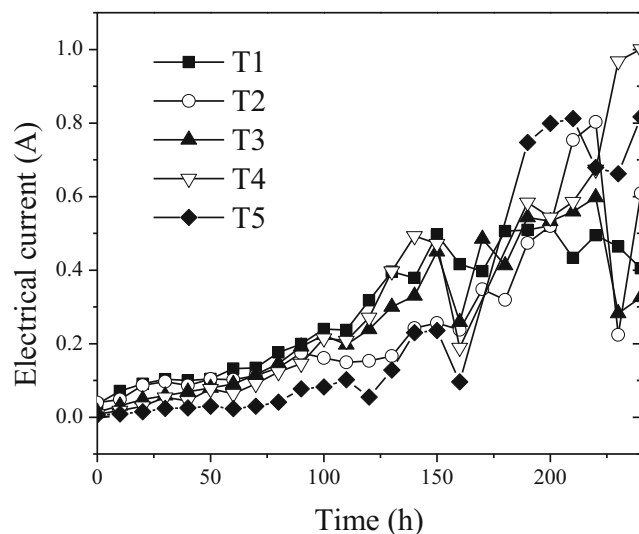


Fig. 3 Changes in electrical current in different treatments

160 to 200 h, which was attributed to the more anode cells (injection locations) in T5. After electrolyte was added, the current would increase sharply in a short time, then decrease as the ions migrate to anode and cathode. Theoretically, a larger current corresponds to a stronger electric field strength, which is beneficial to the migration of oxidants into the system through electroosmotic flow, thereby promoting the degradation of organic contaminants.

Change in soil solution pH

Figure 4 shows the change in pH of soil solution in different treatments. The overall trend in soil solution change was acidification near the anode and alkalization near the cathode, and the area of the alkalized region was larger than that of the acidified region, which was related to the higher initial soil pH (8.42). The change in pH in the soil solution of T1 and T2 was basically the same. As the experiment progressed, the H^+ produced by the anode and the OH^- generated by the cathode continued to diffuse into the system until the two ions met. However, the pH of the soil solution in T1 changed slightly faster than that in T2. After 5 days, the pH of the soil solution near the anode dropped to below 1 and the pH of the soil solution near the cathode increased to above 12 (Fig. 4). The difference in soil solution pH between T1 and T2 may be related to the heterogeneity of soil (Risco et al. 2016e).

In T3, T4, and T5, the anodes were at the top corner and the cathode was at the center, so the acidic region spread from the top corner to the center and the alkaline region spread from the center to the surroundings. Theoretically, the migration rate of H^+ is 1.8 times that of OH^- (Acar and Alshawabkeh 1993). However, in T3, T4, and T5, the pH of soil solution near the cathode was significantly alkalized on day 3 (not shown in Fig. 3), while the pH of the soil solution near the anode was obviously decreased on days 5 and 10. These results were attributed to the higher soil pH (8.42). However, the current at the cathode was several times that at the anode (three times in T3, four times in T4, and six times in T5) (Fan et al. 2007), which was also an important reason for the large proportion of the alkaline soil solution. Comparison of T3, T4, and T5 revealed that, as the number of anodes increased, the acidified area of the soil solution increased.

Change in $\text{S}_2\text{O}_8^{2-}$ concentration of soil solution

The changes in $\text{S}_2\text{O}_8^{2-}$ concentrations in each treatment are shown in Fig. 5. In T1, as the experiment progressed, the concentration of $\text{S}_2\text{O}_8^{2-}$ diffused into the soil increased continuously, and the diffusion area also increased. A study conducted by Fan et al. (2014a) showed that for persulfate anion, electroosmotic flow was more effective than electromigration. The concentration of $\text{S}_2\text{O}_8^{2-}$ was highest in the system at the end of the experiment, and the highest

Fig. 4 Change in pH of soil solution in different treatments

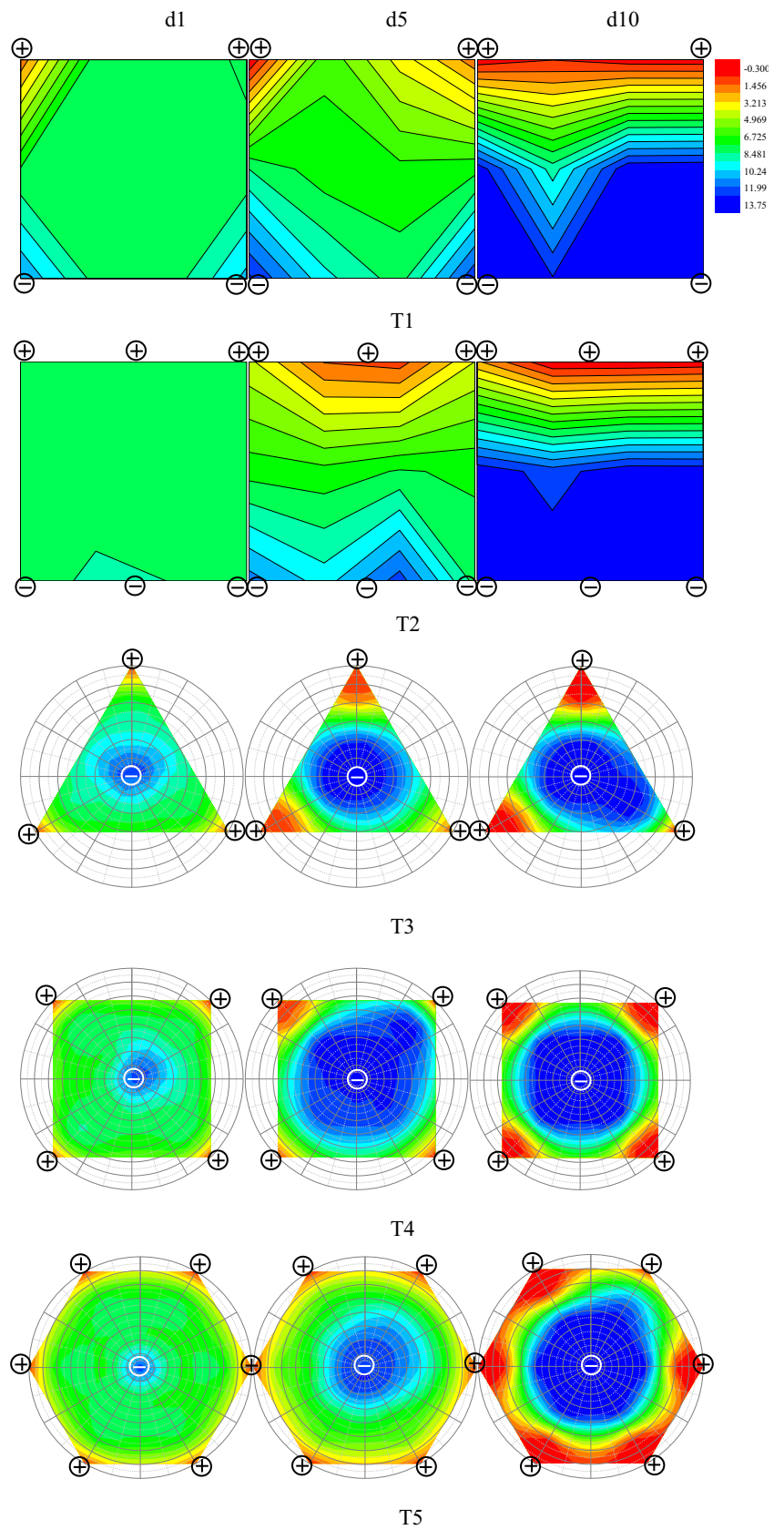
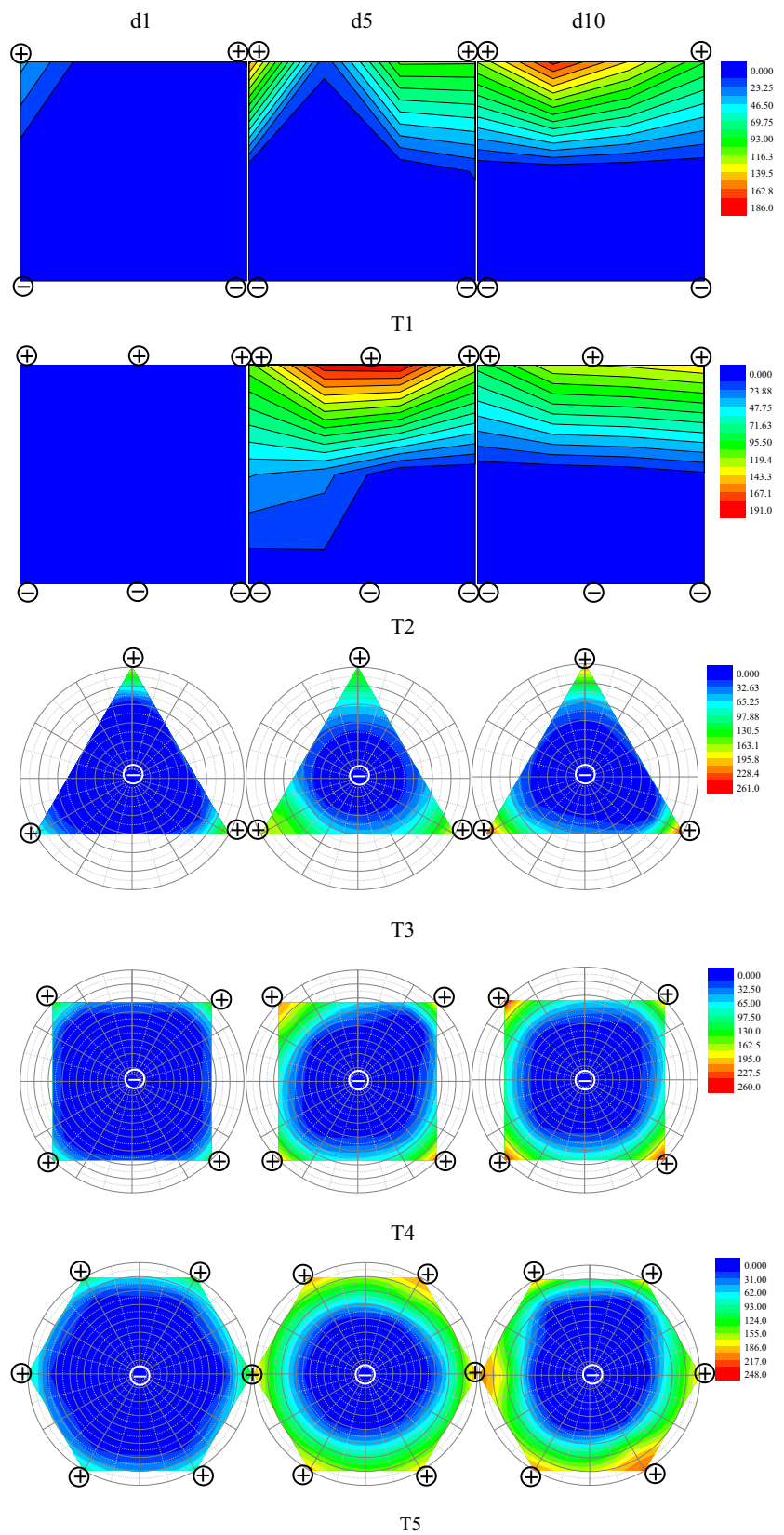


Fig. 5 Change in $S_2O_8^{2-}$ concentration ($mg L^{-1}$) of soil solution in different treatments



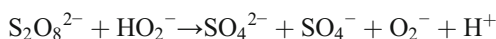
concentration of $S_2O_8^{2-}$ found in the solution was $178.9 g L^{-1}$. In T2, one more anode oxidant dosing site was

added compared to T1, so the oxidant diffused faster than T1. However, the maximum diffusion area of the oxidant entering

the system was observed on day 5, while the maximum concentration reached 191.0 g L^{-1} and the area decreased at the end of the experiment (day 10). This may be attributed to the acid solution pH (Fig. 4) leading to weakened or even reversed electroosmotic flow (Zhou et al. 2004).

In the 2D electrode configurations, although there were more dosing sites than in the 1D systems, the transmission of oxidants into the system was still not improved. The comparison of T3, T4, and T5 showed that with the increase of the number of anodes, the oxidant dose transporting into the system also increased. When compared with T3 and T4, the oxidant diffusion area of T5 increased, and the highest concentration of oxidant was 162.5 g L^{-1} . This can be attributed to an increase in the oxidant dosing site and an increase in the acidified area. The studies of Fan et al. (2014a) and Xu et al. (2020) had proved that the pH values of soil solution in EK+ persulfate treatment were lower than those in only EK treatment.

Generally, the hydrolysis of persulfate generated sulfate ion (SO_4^{2-}), hydrogen ion (H^+), perhydroxyl radical (HO_2^\cdot), sulfate radicals (SO_4^\cdot), and superoxide radicals (O_2^\cdot) in the following equations (Wang and Wang 2018):



At alkaline condition, perhydroxyl radicals tend to decompose into hydroxyl radicals, and sulfate radicals further transformed into hydroxyl radicals, while at acid condition, superoxide radicals tend to react with hydrogen ion to form perhydroxyl radicals (Yang et al. 2014). So the change of $\text{S}_2\text{O}_8^{2-}$ concentration was related to the change of pH of the soil solution. The higher the pH of the soil solution, the lower the concentration of $\text{S}_2\text{O}_8^{2-}$. This was because $\text{S}_2\text{O}_8^{2-}$ was easily activated and decomposed under alkaline conditions. $\text{S}_2\text{O}_8^{2-}$ can be activated by alkaline conditions to produce OH^\cdot (Liang and Lee 2012). Although OH^\cdot has strong oxidizing properties, it is unstable and easy to quench. In addition, the hydrolysis of persulfate generated hydrogen ion and tend to the pH decrease of soil solution.

Soil pH and EC after restoration

Based on the pH distribution in Fig. 6, the overall trend of soil pH was that the pH decreased near the anode and increased near the cathode. The average soil pH values in T1–T5 were 7.94, 7.00, 8.40, 8.30, and 7.87, respectively, after the EK tests (Table 2), which were lower than the initial soil pH (8.42). Comparison of T1 and T2 revealed that the acidification of the soil in T2 (pH = 7.00) was more obvious than that of T1 (pH = 7.94), which corresponded to the migration of persulfate in soil because the decomposition of persulfate could decrease the soil pH. In addition, the increasing pairs

of electrodes promoted soil acidification by the hydrolysis in the anode region and the migration of H^+ in the 1D electrode configurations.

In the 2D electrode configurations, increasing the electrodes could also promote an increase in the soil acidification area, and the acidified area of T5 was larger than that of T3 and T4. However, the alkaline area accounts for a large proportion of the 2D electrode configurations and the soil pH around the central electrode changed more significantly than that near the peripheral electrodes. Fan et al. (2007) also found similar phenomena. This may have been because the current through the central electrode was theoretically several times (three times in T3, four times in T4 and six times in T5) as large as that passing through the individual peripheral electrode, which produced more OH^- in the central cathode and resulted in a larger alkaline area in the 2D electrode configurations.

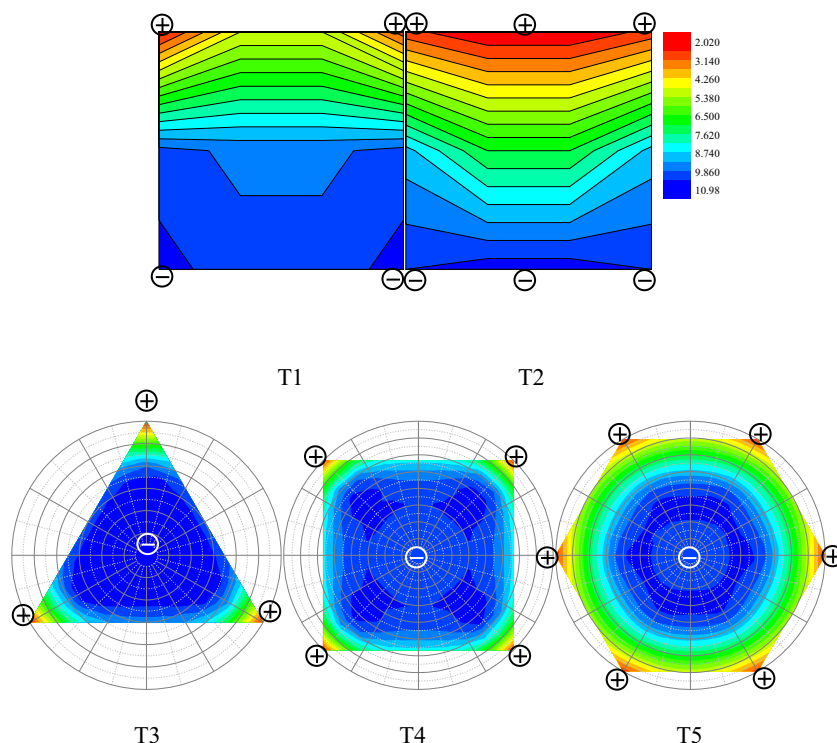
The average soil ECs in T1–T5 were 6.04, 7.52, 9.12, 9.08, and 11.73 mS cm^{-1} , respectively (Table 2), which were higher than the initial soil EC (0.3 mS cm^{-1}). The soil EC reflects the content of mobile ions in the soil (Kim et al. 2012a), and increases in EC also demonstrate increases in the salt content, which is an important indicator that affects the soil reutilization. With the addition of oxidant in each treatment, the soil EC values increased significantly. As shown in Fig. 7, in 1D electrode configurations, as the electrode pairs increased, the EC also increased. The overall soil ECs of the 2D electrode configurations were higher than those of the 1D electrode configurations, which was related to the presence of more anode sites and oxidant dosing sites in the 2D electrode configurations.

The change in soil ECs was consistent with the trend of pH change, following the rule that a lower pH was associated with a higher EC. Lower soil pH would promote the dissolution of soil minerals (carbonate mineral, etc.) and the desorption of some base ions (Ca^{2+} , Mg^{2+} , etc.), reduce the precipitation of metal ions, and then increase the EC of the system (Zhou et al. 2004). In the 1D electrode configuration, the acidified area of T2 was larger than that of T1, so its EC was higher, especially near the anode, and the maximum EC value could reach 15.8 mS cm^{-1} . In the 2D electrode configuration, the EC of the hexagonal configuration increased most significantly.

Removal rate and distribution of PAHs after remediation

The distribution of PAHs after remediation is shown in Fig. 8 and Table 1. The total removal rate of PAHs in T1 was 0.54%, but the removal rate near the anode reached 52.5%. This was because of the higher oxidant concentration near the anode, which could effectively degrade the PAHs. However, the strongly acidic environment near the anode also promoted the degradation of PAHs (Cang et al. 2013). The lowest

Fig. 6 Soil pH after different treatments



removal rate near the cathode in T1 was -46.4% (from initial concentration 6.69 mg kg^{-1} to the final concentration 9.80 mg kg^{-1}), suggesting that PAHs migrated toward the cathode via electroosmotic flow and then accumulated there. Maini et al. (2000) also demonstrated that PAHs migrated from the anode to the cathode under an electric field. Similarly, in the 1D electric field, the total removal rate of PAHs in T2 was much higher than that in T1, with 31.6% of PAHs removed. In T2, the PAHs accumulated at a certain position between the anode and the cathode (see Fig. 7) because the migration of $\text{S}_2\text{O}_8^{2-}$ was weakened or even reversed after day 5 (see Fig. 4).

Compared with the 1D electrode configurations, the removal rates of PAHs in the 2D electrode configurations were improved. The total removal rate of T3 was 35.9% . The removal rate at the anode was highest, reaching 73.4% , and the PAHs accumulated at the cathode. The removal rate of T4 reached 38.7% , and the removal rate of T5 was highest, reaching 40.9% . Although oxidants were not detected in the soil solution near the cathodes of T4 and T5 (see Fig. 4), there

were high PAH removal rates of 29.3% and 44.6% near the cathodes, respectively. This may have been because some organic substances can react with OH^- under strong alkaline conditions, resulting in the decomposition or partial degradation of organic substances (Jeffers et al. 1989). The results reported by Maini et al. (2000) differed from ours. Specifically, they found that the removal of PAHs from the soil occurred regardless of the position of the soil with respect to the alignment of the electrodes in their larger scale electrokinetic remediation of historically contaminated soil. This can be attributed to the longer remediation time and the addition of non-ionic surfactants.

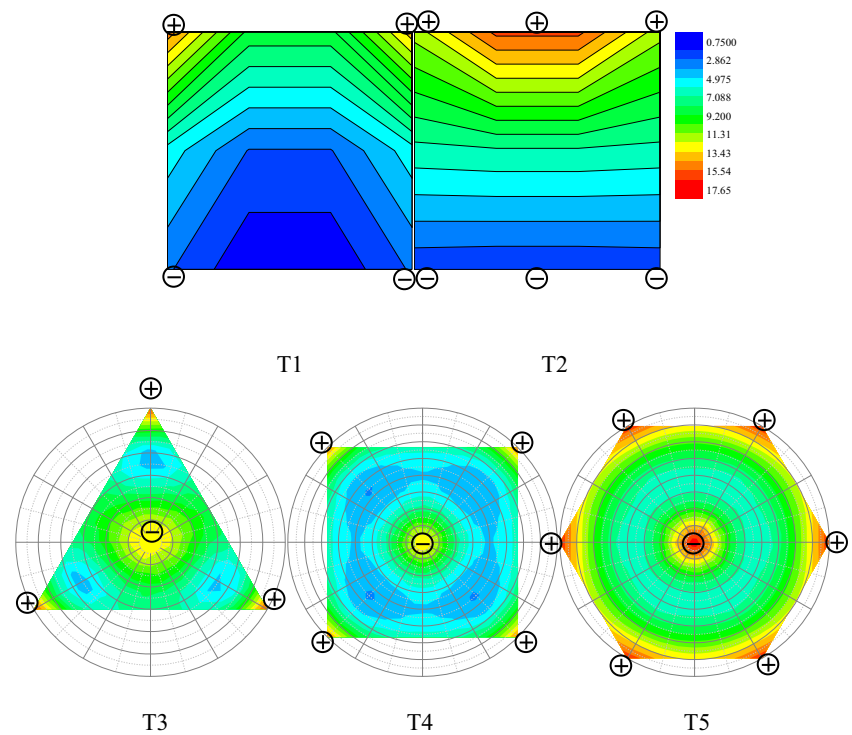
Table 1 shows the removal rate of 16 kinds of PAH in the soil after remediation. There were differences in the degradability of PAHs with different numbers of benzene rings, with PAHs containing more rings generally being more difficult to degrade. This is not only related to the stability of the PAHs, but also to the increased hydrophobicity of PAHs with more benzene rings, which makes them easier to be adsorbed by soil particles and therefore more difficult to contact with oxidants and be oxidized (Watts et al. 2002). Therefore, the PAH removal rate was related to the reactivity of different types of PAHs (Brown et al. 2003), as well as to the soil properties (Jonsson et al. 2007).

The removal rates of fluorene (FLE) and dibenz(a,h)anthracene (DahA) in each treatment group were negative, indicating that the concentration of the FLE and DahA increased after remediation. FLE has few benzene rings and a simple structure; therefore, its accumulation may be

Table 2 Average soil pH and electroconductivity of different treatment groups

	Initial	T1	T2	T3	T4	T5
pH	8.42	7.94	7.00	8.40	8.30	7.87
EC (mS/cm)	0.30	6.04	7.52	8.12	9.08	11.7

Fig. 7 Soil EC (mS cm^{-1}) after different treatments



caused by the degradation and conversion of other PAHs (Watts et al. 2002). DahA is a pentacyclic PAH; therefore, it was more difficult to degrade. The increase in its concentration after remediation may have been because of the uneven distribution of pollutants in the soil.

Power consumption of each treatment group

Table 3 reflects the power consumption of each treatment group. Electrical energy consumption during EK was highly dependent on the number of electrodes, operating time, and

Fig. 8 Distribution of PAH concentration (mg kg^{-1}) in soil after different treatments

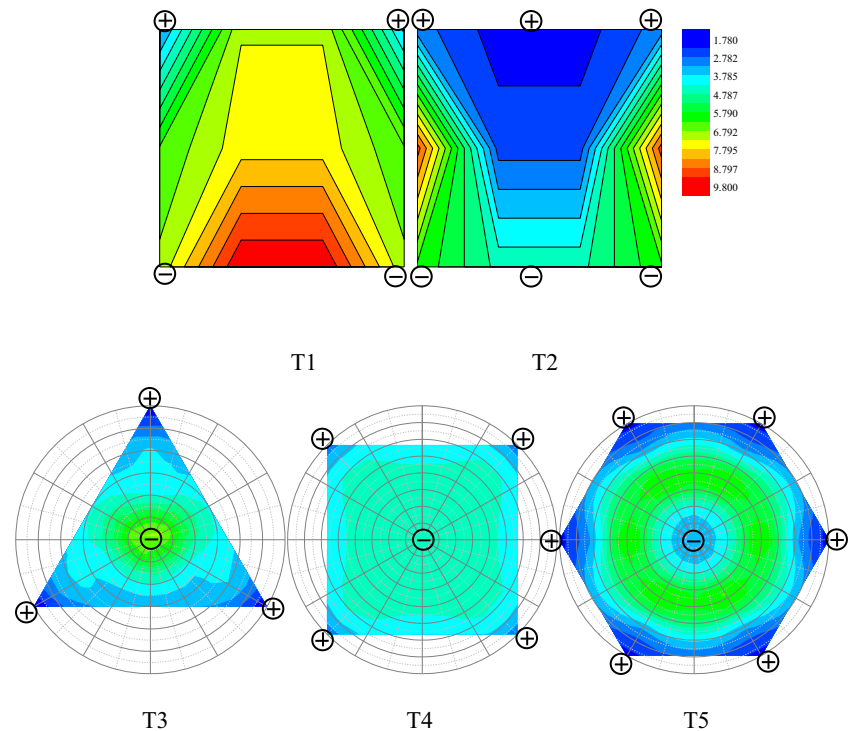


Table 3 Power consumption of different treatment groups

	Removal rate (%)	Removed PAHs (g t ⁻¹)	Total energy consumption (kWh t ⁻¹)	Energy consumption per unit of removal rate (kWh t ⁻¹ % ⁻¹)	Energy consumption per gram removed PAHs (kWh g PAHs ⁻¹)
T1	0.54	0.04	285.5	528	7139
T2	31.6	2.12	241.8	7.66	114.1
T3	35.9	2.40	188.2	5.24	78.41
T4	38.7	2.59	220.8	5.70	85.24
T5	40.9	2.74	182.9	4.48	66.74

voltage gradient applied (Krcmar et al. 2018). The results revealed that the 2D electrode configurations reduced power consumption compared to 1D electrode configurations in both energy consumption per unit of removal rate and energy consumption per gram removed PAHs. Kim et al. (2012a) found that a hexagonal electrode system was more effective at restoring saline soil, in terms of both salt removal and energy consumption, than a system with 1D electrodes. Kim et al. (2014) found that 2D was more efficient than 1D for remediation of an equal volume of contaminated soil using low daily energy consumption and fewer electrodes.

In T3, T4, and T5, there were no significant differences in total energy consumption and energy consumption per unit removal rate, indicating that increasing the number of anodes would not cause an increase in energy consumption in 2D electrode configurations. In all treatment groups, the hexagonal electrode configuration had the lowest total energy consumption (182.9 kWh t⁻¹) and energy consumption per unit removal rate (4.48 kWh t⁻¹%⁻¹) and energy consumption per gram removed PAHs (66.74 kWh (g PAHs)⁻¹). However, increasing the number of anodes would also increase the costs for fabrication and installation of electrodes (Alshawabkeh et al. 1999). Therefore, the appropriate electrode configuration should be selected in consideration of the cost and removal rate in practical applications.

Conclusions

During EK-enhanced persulfate oxidation remediation under different electrode configurations, increasing the number of anodes and electrode pairs in 1D and 2D electrode configurations facilitated diffusion of oxidants in soil. The soil pH and EC changed obviously and the soil ECs in the 2D electrode configuration treatments were higher than in 1D electrode configuration treatments. From the perspective of PAH removal rates in different treatments, 2D electrode configurations had higher removal rates of PAHs (35.9–40.9%) than 1D electrode configurations (0.54–31.6%), and the hexagonal electrode configuration had the highest removal efficiency in all treatments, with PAH removals of up to 40.9%. From the perspective of PAH distribution in the soil after remediation,

the acidic environment around the anode and the alkaline environment around the cathode were both conducive to the removal of PAHs. In terms of energy consumption, 2D electrode configurations consumed less power than 1D configurations, and the hexagonal electrode configuration had the lowest energy consumption per unit removal rate (4.48 kWh t⁻¹%⁻¹) in all electrode configurations. However, the transport of oxidants and removal efficiency of organic pollutants were still not sufficient; therefore, further studies are needed to determine how to increase efficiency.

Funding information This research was financially supported by the National Key R&D Program of China (Grant Nos. 2018YFC1802005) and the Natural Science Foundation of China (41471261).

Compliance with ethical standards

Conflict of interest The authors declare that they have no competing interests.

References

- Acar YB, Alshawabkeh AN (1993) Principles of electrokinetic remediation. *Environ Sci Technol* 27:638–2647
- Alshawabkeh AN, Yeung AT, Bricka MR (1999) Practical aspects of in-situ electrokinetic extraction. *J Environ Eng* 125:27–35
- Bento FM, Camargo FAO, Okeke BC, Frankenberger WT (2005) Comparative bioremediation of soils contaminated with diesel oil by natural attenuation, biostimulation and bioaugmentation. *Bioresour Technol* 96:1049–1055
- Barba S, Villasenor J, Rodrigo MA, Canizares P (2017) Effect of the polarity reversal frequency in the electrokinetic-biological remediation of oxyfluorfen polluted soil. *Chemosphere* 177:120–127
- Brown GS, Barton LL, Thomson BM (2003) Permanganate oxidation of sorbed polycyclic aromatic hydrocarbons. *Waste Manag* 23:737–740
- Cang L, Fan GP, Zhou DM, Wang QY (2013) Enhanced-electrokinetic remediation of copper-pyrene co-contaminated soil with different oxidants and pH control. *Chemosphere* 90:2326–2331
- Dermont G, Bergeron M, Mercier G, Richer-Lafleche M (2008) Soil washing for metal removal: a review of physical/chemical technologies and field applications. *J Hazard Mater* 152:1–31
- Fan GP, Cang L, Fang GD, Zhou DM (2014a) Electrokinetic delivery of persulfate to remediate PCBs polluted soils: effect of injection spot. *Chemosphere* 117:410–418

- Fan GP, Cang L, Fang GD, Zhou DM (2014b) Surfactant and oxidant enhanced electrokinetic remediation of a PCBs polluted soil. *Sep Purif Technol* 123:106–113
- Fan X, Wang H, Luo Q, Ma JW, Zhang XH (2007) The use of 2D non-uniform electric field to enhance in situ bioremediation of 2,4-dichlorophenol-contaminated soil. *J Hazard Mater* 148:29–37
- Ferrarese E, Andreottola G, Oprer IA (2008) Remediation of PAH-contaminated sediments by chemical oxidation. *J Hazard Mater* 152:128–139
- Fu RB, Wen DD, Xia X, Zhang W, Gu YY (2017) Electrokinetic remediation of chromium (Cr)-contaminated soil with citric acid (CA) and polyaspartic acid (PASP) as electrolytes. *Chem Eng J* 316:601–608
- Gryzenia J, Cassidy D, Hampton D (2009) Production and accumulation of surfactants during the chemical oxidation of PAH in soil. *Chemosphere* 77:540–545
- Jeffers PM, Ward LM, Woytowitch LM, Wolfe NL (1989) Homogeneous hydrolysis rate constants for selected chlorinated methanes, ethanes, ethenes, and propanes. *Environ Sci Technol* 23:965–969
- Jonsson S, Persson Y, Frankki S, van Bavel B, Lundstedt S, Haglund P, Tysklind M (2007) Degradation of polycyclic aromatic hydrocarbons (PAHs) in contaminated soils by Fenton's reagent: a multivariate evaluation of the importance of soil characteristics and PAH properties. *J Hazard Mater* 149:86–96
- Juhasz AL, Naidu R (2000) Bioremediation of high molecular weight polycyclic aromatic hydrocarbons: a review of the microbial degradation of benzo[a]pyrene. *Int Biodeterior Biodegrad* 45:57–88
- Kim DH, Jo SU, Choi JH, Yang JS, Baek K (2012a) Hexagonal two dimensional electrokinetic systems for restoration of saline agricultural lands: a pilot study. *Chem Eng J* 198–199:110–121
- Kim WS, Jeon EK, Jung JM (2014) Field application of electrokinetic remediation for multi-metal contaminated paddy soil using two-dimensional electrode configuration. *Environ Sci Pollut Res* 21:4482–4491
- Kim WS, Park GY, Kim DH, Jung HB, Ko SH, Baek K (2012b) In situ field scale electrokinetic remediation of multi-metals contaminated paddy soil: influence of electrode configuration. *Electrochim Acta* 86:89–95
- Krcmar D, Varga N, Prica M, Cveticanin L, Zukovic M, Dalmacija B, Corba Z (2018) Application of hexagonal two dimensional electrokinetic system on the nickel contaminated sediment and modelling the transport behavior of nickel during electrokinetic treatment. *Sep Purif Technol* 192:253–261
- Liang C, Huang CF, Chen YJ (2008a) Potential for activated persulfate degradation of BTEX contamination. *Water Res* 42:4091–4100
- Liang C, Lee PH (2012) Granular activated carbon/pyrite composites for environmental application: synthesis and characterization. *J Hazard Mater* 231–232:120–126
- Liang C, Huang CF, Mohanty N, Kurakalva RM (2008b) A rapid spectrophotometric determination of persulfate anion in ISCO. *Chemosphere* 73:1540–1543
- Lopez-Vizcaino R, Yustres A, Saez C, Canizares P, Rodrigo MA, Navarro V (2017) Effect of polarity reversal on the enhanced electrokinetic remediation of 2,4-D-polluted soils: a numerical study. *Electrochim Acta* 258:414–422
- Lu RK (2000) Analysis methods of soil agricultural chemistry. Agricultural Science Press, Beijing (in Chinese)
- Maini G, Sharman AK, Knowles CJ, Sunderland G, Jackman SA (2000) Electrokinetic remediation of metals and organics from historically contaminated soil. *J Chem Technol Biotechnol* 75:657–664
- Mena E, Villasenor J, Rodrigo MA, Canizares P (2016) Electrokinetic remediation of soil polluted with insoluble organics using biological permeable reactive barriers: effect of periodic polarity reversal and voltage gradient. *Chem Eng J* 299:30–36
- Pies C, Hoffmann B, Petrowsky J, Yang Y, Termes TA, Hofmann T (2008) Characterization and source identification of polycyclic aromatic hydrocarbons (PAHs) in river bank soils. *Chemosphere* 72:1594–1601
- Rastogi A, Al-Abed SR, Dionysiou DD (2009a) Effect of inorganic, synthetic and naturally occurring chelating agents on Fe(II) mediated advanced oxidation of chlorophenols. *Water Res* 43:684–694
- Rastogi A, Al-Abed SR, Dionysiou DD (2009b) Sulfate radical-based ferrous-peroxymonosulfate oxidative system for PCBs degradation in aqueous and sediment systems. *Appl Catal B Environ* 85:171–179
- Risco C, Rodrigo S, Vizcaino RL, Yustres A, Saez C, Canizares P, Navarro V, Rodrigo MA (2016a) Removal of oxyfluorfen from spiked soils using electrokinetic soil flushing with linear rows of electrodes. *Chem Eng J* 294:65–72
- Risco C, Lopez-Vizcaino R, Saez C, Yustres A, Canizares P, Navarro V, Rodrigo MA (2016b) Remediation of soils polluted with 2,4-D by electrokinetic soil flushing with facing rows of electrodes: a case study in a pilot plant. *Chem Eng J* 285:128–136
- Risco C, Rubi-Juarez H, Rodrigo S, Lopez-Vizcaino R, Saez C, Canizares P, Barrera-Diaz C, Navarro V, Rodrigo MA (2016c) Removal of oxyfluorfen from spiked soils using electrokinetic soil flushing with the surrounding arrangements of electrodes. *Sci Total Environ* 559:94–102
- Risco C, Rodrigo S, Lopez-Vizcaino R, Saez C, Canizares P, Navarro V, Rodrigo MA (2016d) Electrokinetic flushing with surrounding electrode arrangements for the remediation of soils that are polluted with 2,4-D: a case study in a pilot plant. *Sci Total Environ* 545:256–265
- Risco C, Rubi-Juarez H, Rodrigo S, Vizcaino RL, Saez C, Canizares P, Barrera-Diaz C, Navarro V, Rodrigo MA (2016e) Removal of oxyfluorfen from spiked soils using electrokinetic fences. *Sep Purif Technol* 167:55–62
- Saichek RE, Reddy KR (2003) Effect of pH control at the anode for the electrokinetic removal of phenanthrene from kaolin soil. *Chemosphere* 51:273–287
- Sawada A, Mori K, Tanaka S, Fukushima M, Tatsumi K (2004) Removal of Cr(VI) from contaminated soil by electrokinetic remediation. *Waste Manag* 24:483–490
- Tang L, Tang XY, Zhu YG, Zheng MH, Miao QL (2005) Contamination of polycyclic aromatic hydrocarbons (PAHs) in urban soils in Beijing, China. *Environ Int* 31:822–828
- Tsitonaki A, Petri B, Crimi M, Mosbaek H, Siegrist RL, Bjerg PL (2010) In situ chemical oxidation of contaminated soil and groundwater using persulfate: a review. *Crit Rev Environ Sci Technol* 10:55–91
- Turer D, Genc A (2005) Assessing effect of electrode configuration on the efficiency of electrokinetic remediation by sequential extraction analysis. *J Hazard Mater* 119:167–174
- Wang J, Wang S (2018) Activation of persulfate (PS) and peroxymonosulfate (PMS) and application for the degradation of emerging contaminants. *Chem Eng J* 334:1502–1517
- Watts RJ, Stanton PC, Howsawkeng J, Teel AL (2002) Mineralization of a sorbed polycyclic aromatic hydrocarbon in two soils using catalyzed hydrogen peroxide. *Water Res* 36:4283–4292
- Xu HT, Song Y, Cang L, Zhou DM (2020) Ion exchange membranes enhance the electrokinetic in situ chemical oxidation of PAH-contaminated soil. *J Hazard Mater* 382:121042
- Yang GCC, Yeh CF (2011) Enhanced nano-Fe₃O₄/S₂O₈²⁻ oxidation of trichloroethylene in a clayey soil by electrokinetics. *Sep Purif Technol* 79:264–271
- Yang Y, Pignatello JJ, Ma J, Mitch WA (2014) Comparison of halide impacts on the efficiency of contaminant degradation by sulfate and hydroxyl radical-based advanced oxidation processes (AOPs). *Environ Sci Technol* 48:2344–2351
- Yang K, Zhu L, Xing B (2006) Enhanced soil washing of phenanthrene by mixed solutions of TX100 and SDBS. *Environ Sci Technol* 40:4274–4280

- Yukselen-Aksoy Y, Reddy KR (2012) Effect of soil composition on electrokinetically enhanced persulfate oxidation of polychlorobiphenyls. *Electrochim Acta* 86:164–169
- Yu JW, Neretnieks I (1997) Theoretical evaluation of a technique for electrokinetic decontamination of soils. *J Contam Hydrol* 26:291–299
- Zhang Y, Chu G, Dong P, Xiao J, Meng Q, Baumgartel M, Xu B, Hao T (2018) Enhanced electrokinetic remediation of lead- and cadmium-contaminated paddy soil by composite electrolyte of sodium chloride and citric acid. *J Soils Sediments* 18:1915–1924
- Zhao C, Dong Y, Feng YP, Li YZ, Dong Y (2019) Thermal desorption for remediation of contaminated soil: a review. *Chemosphere* 221:841–855
- Zhou DM, Deng CF, Cang L (2004) Electrokinetic remediation of a Cu contaminated red soil by conditioning catholyte pH with different enhancing chemical reagents. *Chemosphere* 56:265–273
- Zhou DM, Deng CF, Cang L, Alshawabkeh AN (2005) Electrokinetic remediation of a Cu–Zn contaminated red soil by controlling the voltage and conditioning catholyte pH. *Chemosphere* 61:519–527
- Zhou DM, Chen HF, Cang L, Wang Y (2007) Ryegrass uptake of soil Cu/Zn induced by EDTA/EDDS together with a vertical direct-current electrical field. *Chemosphere* 67:1671–1676

Publisher's note Springer Nature remains neutral with regard to jurisdictional claims in published maps and institutional affiliations.